

# Ultrafast Charge Transfer at $\text{TiO}_2/\text{SCN}^-$ (aq) Interfaces Investigated by Femtosecond Transient Reflecting Grating Method

Tomohiro Morishita, Akihide Hibara, and Tsuguo Sawada\*

Department of Applied Chemistry, School of Engineering, The University of Tokyo, 7-3-1 Hongo, Bunkyo-ku, Tokyo 113-8656, Japan

Isao Tsuyumoto

Department of Environmental Systems Engineering, Kanazawa Institute of Technology, 7-1 Ohgigaoka, Nonoichi, Ishikawa 921-8501

Received: December 14, 1998; In Final Form: May 23, 1999

We applied a femtosecond transient reflecting grating (TRG) method to solid/liquid interfaces to successfully observe the photoinduced ultrafast relaxation dynamics at  $\text{TiO}_2(001)/\text{KSCN}$  (aq) interfaces. We found, for the first time, an ultrafast relaxation component (110–690 fs). The component intensity clearly increases with increasing concentration of KSCN, and it is strongly dependent on the number of photoexcited carriers. We concluded that this component is due to the interaction between photoinduced nonequilibrium holes and adsorbed  $\text{SCN}^-$  ions and that ultrafast charge transfer occurs by way of this interaction. These results suggest a new ultrafast charge transfer process involving nonequilibrium carriers.

## Introduction

The charge carrier dynamics at solid/liquid interfaces plays a crucial role in various processes such as electrode reactions, photocatalysis, photosynthesis, and corrosion.<sup>1–5</sup> Understanding the ultrafast charge transfer dynamics at the interfaces is fundamentally important for designing functional electrode surfaces and for controlling the interfacial reactions. Over the years, a number of experimental techniques have been developed to investigate the static structures and the dynamic properties of solid/liquid interfaces.<sup>6–8</sup> Among these, a transient grating method is a versatile technique which combines high time resolution, interfacial selectivity, high sensitivity, and in situ measurements.<sup>9,10</sup> This method utilizes nonradiative relaxation processes of electrons, while fluorescence (luminescence) spectroscopy utilizes radiative relaxation processes, and measurements of unmodified interfaces are possible because it does not require luminescence or fluorescence in situ.

We have extended a transient reflecting grating (TRG) method to the femtosecond time region and have applied it to solid surfaces. We successfully monitored the energy dissipation processes of hot electrons on gold surfaces<sup>11</sup> and the carrier transport dynamics on silicon surfaces.<sup>12</sup> The TRG method has an advantage over the conventional transient reflecting (TR) method because it can provide directional dynamic properties with a much higher  $S/B$  (signal to background) ratio.

Recently, the contribution of nonthermalized electrons in photoexcited reaction systems has attracted much attention. The electrons which are not in equilibrium with other electrons and phonons are generally called hot electrons. We have observed an interaction having a relaxation time of 20 fs between photoexcited electrons and adsorbed solute anions at a platinum/electrolyte interface using the TR method.<sup>13</sup> We presumed that this ultrafast interaction is due to nonthermalized electrons (NTEs).

In this study we applied the femtosecond TRG method to  $\text{TiO}_2/\text{KSCN}$  (aq) interfaces. Although a number of researchers have reported on the dynamics of the photoexcited reaction of  $\text{TiO}_2$ , their focus has mainly been on electron–hole recombination processes on a time scale of 10 ps to 100 ns.<sup>14–17</sup> There are indeed few reports which deal with photoexcited carriers within a time scale of 1 ps. Among these, Hannappel et al.<sup>18</sup> have reported an ultrafast photoinduced electron transfer from chemically anchored Ru–dye to a colloidal anatase  $\text{TiO}_2$  film within 25 fs. This electron transfer occurred after excitation of dye molecules, which is of practical importance in a functional solid surface such as in a solar cell. In the following, we focus on the behavior of hot carriers after excitation of the  $\text{TiO}_2$  phase at  $\text{TiO}_2/\text{KSCN}$  (aq) interfaces. Our aim is to elucidate the contribution of nonequilibrium carriers to the photoexcited interfacial reaction of  $\text{TiO}_2$ . We describe an ultrafast relaxation 110–690 fs after the excitation of  $\text{TiO}_2$  at the interface and propose a new type of charge transfer which explains the limits of the applicability of conventional theory.

## Experimental Section

The experimental setup for the TRG measurements was the same as that described in our previous report,<sup>19</sup> except for the sample arrangement for the solid/liquid interface measurements. An outline follows here. The sample surface is irradiated by two pump pulses of the same wavelength  $\lambda_{\text{pump}}$ , and an optical interference pattern is formed on it. This interference pattern transforms into a periodical refractive index change, which acts as a transient diffraction grating. A probe pulse is incident normal to the grating, and diffracted light is observed. The intensity of the diffracted light is monitored as a function of the delay time of the probe beam. The TRG signal reflects dynamic information on surfaces such as refractive index change by electronic excitation and surface displacement by heat generation.

\* To whom any correspondence should be addressed.

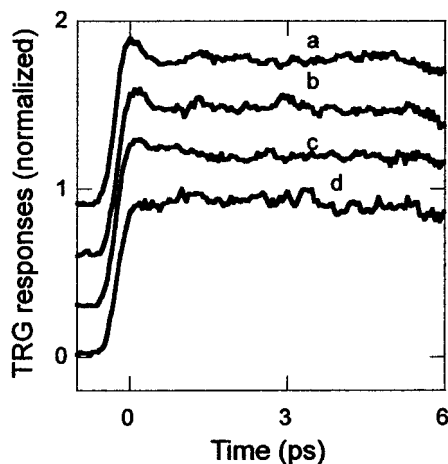


**Figure 1.** Typical TRG signals from  $\text{TiO}_2/\text{SCN}^-$  (aq) interfaces with various  $\text{SCN}^-$  concentrations. The concentrations of  $\text{SCN}^-$  are (a) 20; (b) 15; (c) 10, and (d) 0 mM. For clarity, the signals are vertically displaced.

The light source was a regeneratively amplified Ti:sapphire laser system which had an autocorrelation of 150 fs, a wavelength of 800 nm, and a repetition rate of 1 kHz. The output beam of the 800 nm wavelength was partly reflected by a half mirror to generate a probe beam passing through a computer-controlled optical delay line. The residual beam was frequency-doubled by a BBO crystal to generate a 400 nm beam which was split into two parts. Each pump pulse had a spot size of  $600 \mu\text{m}$ , and the fluency was changed from 2.16 to 4.57 mJ/cm<sup>2</sup>. The pump pulse had p-polarization. We wanted to study how the photoexcited carrier density affects the interface reaction. The fringe spacing was set to  $2.1 \mu\text{m}$  by setting the incident angle to  $5^\circ$ . Polarizations of the pump and probe beams were perpendicular to each other. The diffracted light was detected by a PIN photodiode. The output of the photodiode was fed into a fast-gated integrator and its average signal was recorded as a TRG response.

We fabricated a sample cell for solid/liquid interface measurements using an optical cell. Its optical window was made of quartz glass with optically flat surfaces, and the thickness of the liquid phase could be controlled by changing the spacers. Controlling the thickness of the liquid phase was indispensable to improvement of the S/N ratio because fluctuation of the liquid phase greatly disturbs the measurement. A solid/liquid interface was prepared by pouring a KSCN (aq) solution into the sample cell. A  $\text{TiO}_2$  single crystal was attached to the sample cell. The  $\text{TiO}_2$  single crystal with rutile structure (001) surfaces was purchased (K & R Creation Co., Inc.) and used without any modification. KSCN was also purchased (Wako Chemical Co., Inc.; special grade, 99.5% purity) and used without further purification. The concentrations of KSCN (aq) solution were in the range 0–20 mM, with a pump beam fluency of 4.5 mJ/cm<sup>2</sup>. We intended to study how the population of adsorbate on  $\text{TiO}_2$  affects the behavior of photoexcited carriers.

## Results and Discussion

TRG responses from the interfaces between  $\text{TiO}_2$  and KSCN (aq) in the range of 0–20 mM are shown in Figure 1. The S/N ratio of the TRG signals was dramatically improved by decreasing the thickness of the liquid phase which prevented its fluctuation. We empirically found that the best S/N ratio was obtained when the thickness was 0.5 mm. In this study, all measurements were performed with 0.5 mm thick liquid phases. The intensity of the TRG signals in the experiments below was

**TABLE 1: Time Constants and Pre-exponential Factors Calculated as Fitting Parameters for the TRG Signals<sup>a</sup>**

pump power intensity (mW)	$t_1$ (fs)	$t_2$ (ps)	$C_1$	$C_2$
4	110	173	0.54	0.46
5	200	137	0.38	0.62
7	450	130	0.22	0.78
8	690	150	0.17	0.83

<sup>a</sup> Concentration of KSCN is fixed at 15 mM.

almost the same, regardless of the thickness of the liquid phase. This indicates that the TRG signals were not from the bulk solutions but from the interface.

First, we discuss the TRG response. An increase in the TRG signal corresponds to the change in the refractive index of the sample surfaces induced by the generation of photoexcited carriers. We assume that the change in the extinction coefficient is negligible at the probe wavelength. The change in the refractive index upon the photoexcitation of electron–hole pairs can be approximated by the Drude model for the optical properties of quasi-free carriers. Therefore, the change in the refractive index  $\Delta n$  is given by

$$\Delta n = \frac{-Ne^2}{2nm_{\text{ch}}\omega_p^2\epsilon_0} \quad (1)$$

where  $N$  is the photoexcited carrier density,  $e$  is the fundamental electron charge,  $m_{\text{ch}}$  is the effective reduced mass of the electron–hole pair, and  $\omega_p$  is the radial probe frequency. A noticeable point in this experiment is that the change in the refractive index due to the holes is expected to be about 1000 times greater than that from the electrons because the effective masses of holes and electrons are  $0.02m_e$  and  $30m_e$ ,<sup>20</sup> respectively. Therefore, the TRG responses are mainly due to the change in the number of the photoexcited holes as a function of the delay time. Based on this assumption, the TRG responses were analyzed below.

The change in the TRG signal reflects the changes in both the real part ( $n$ ) and the imaginary part ( $k$ ) of the refractive index. The TRG method detects the phenomena which cause changes in the complex dielectric constant. For simplicity, we interpret the change in TRG signals as that in  $n$  in this paper, because  $n$  and  $k$  are associated with each other by Kramers–Kronig relations and the change in  $n$  is considered to reflect the same phenomena as that in  $k$ .

In Figure 1, around time zero each signal shows an abrupt rise due to generation of holes followed by an ultrafast small fall and then a gradual decrease. This gradual decrease is due to electron–hole recombination which occurs on a nanosecond time scale.<sup>21</sup> Details of the recombination process remain a controversial issue, but they are not the topic of this paper.

We focus on the ultrafast small fall within 1 ps. In Figure 1, the small fall after the peak at the  $\text{TiO}_2/\text{SCN}^-$  interfaces clearly becomes greater with increasing  $\text{SCN}^-$  concentration and the small fall is never observed at the  $\text{TiO}_2/\text{H}_2\text{O}$  interface. The time constant of this decay component is summarized in Table 1 (see below). The adsorption of  $\text{SCN}^-$  ion is not saturated in this concentration region, and the number of adsorbate ( $\text{SCN}^-$ ) increases with increasing concentration of  $\text{SCN}^-$ .<sup>17</sup> Therefore, the increase in the intensity of the small fall reflects the phenomena involving the adsorbate ( $\text{SCN}^-$ ). The maximum height of the TRG signal is almost constant in all experiments, which suggests that there is no change in the density of pump beam fluency due to self-focusing induced by the  $\text{SCN}^-$  (aq).

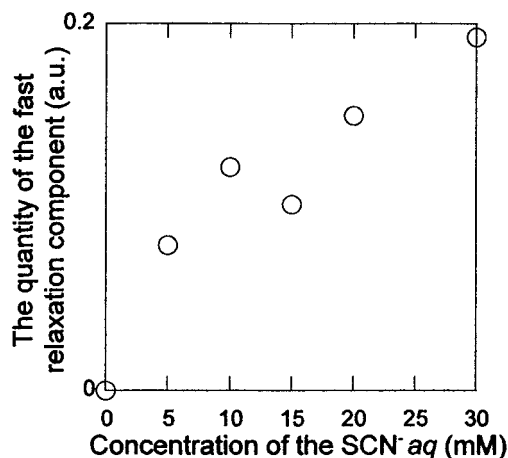


**Figure 2.** Intensity of the ultrafast decay component vs the concentration of SCN<sup>-</sup>. The intensity of the component increases with increasing concentration of SCN<sup>-</sup>.

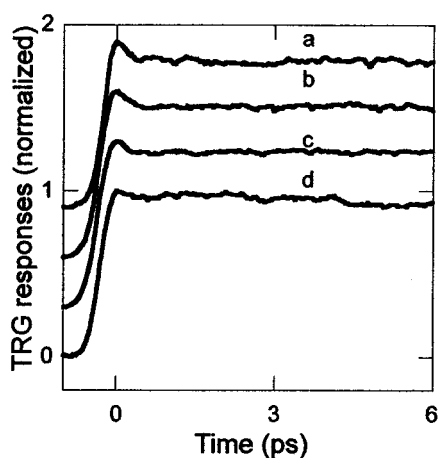


**Figure 3.** Typical TRG signals from the TiO<sub>2</sub>/SCN<sup>-</sup> (aq) interfaces with various pump beam powers. The intensities of the pump beam power are (a) 4; (b) 5; (c) 7; (d) 8 mW. For clarity, the signals are vertically displaced.

These facts indicate that an ultrafast relaxation process of the photoexcited holes within 1 ps occurs at the TiO<sub>2</sub>/SCN<sup>-</sup> (aq) interfaces.

For a detailed analysis of the ultrafast relaxation process, the intensity of the ultrafast decay component vs the concentration of SCN<sup>-</sup> is shown in Figure 2. As we show the next experiment, the relative intensity of the ultrafast relaxation component decreases with increasing pump beam power. Therefore, there is little possibility that this ultrafast relaxation component corresponds to a nonlinear effect induced by SCN<sup>-</sup> ion solution.

In Figure 2, the intensity of the ultrafast decay component increases with the increase of the SCN<sup>-</sup> concentration; that is, the ultrafast relaxation of the photoexcited holes becomes dominant with the increase in the number of adsorbed SCN<sup>-</sup> ions. Thus, we can presume that the observed ultrafast decay is mainly due to ultrafast hole transfer at the interfaces 110–690 fs.

Next, we consider the photoexcited hole dynamics at several pump beam powers. The dependence of the TRG responses from the TiO<sub>2</sub>/SCN<sup>-</sup> interfaces on the number of the photoexcited carriers is shown in Figure 3. The concentration of the SCN<sup>-</sup> (aq) is all 15 mM in this experiment. The atomic density of the TiO<sub>2</sub> is 100 times higher than that of the photoexcited carriers. Therefore, the absorption of the solid sample is not saturated even at high power, and the excitations are all localized in the

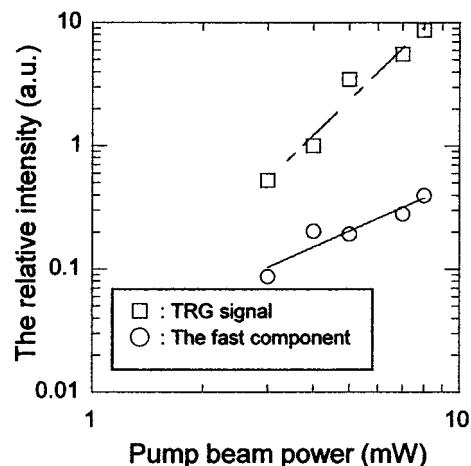


**Figure 4.** Intensity of the TRG signals and the relative intensity of the fast relaxation component vs pump beam power.

same volume. The intensity of the TRG signals and the relative number of the photoexcited carriers which contribute to the interfacial reaction vs the pump beam power is plotted in Figure 4. Both the intensity of the TRG signals and the relative number of the photoexcited carriers increase with the increase of the pump beam power. However, the coefficients of the increase are not as expected. This means that the ratio of the ultrafast charge transfer decreases with an increasing number of photoexcited carriers. This is probably because the path for the ultrafast charge transfer is controlled by not only the density of the photoexcited carriers but also other factors, such as the number of adsorbate molecules and the number of lattice defects at the interface.

The observed TRG signals are fitted with a double exponential decay using a least-squares fitting method. The signals are deconvolved using an instrumental function with fwhm of 250 fs. As shown in Table 1, the time constant increases with increasing the pump beam power (110–690 fs), whereas the intensity decreases with increasing the pump beam power. The increase in the time constants is probably due to the change in path for the ultrafast charge transfer as discussed above.

It is known that photoexcited holes exist as nonequilibrium holes on a time scale of 100 fs after which they undergo an energy dissipation process due to the carrier–carrier scattering process. Our experimental results suggest a role for nonequilibrium holes in the reaction at the TiO<sub>2</sub>/SCN<sup>-</sup> interfaces. With the increase in the number of photoexcited carriers, the energy dissipation process becomes dominant and the interfacial reactive process occurs less, because the rate of the carrier–carrier scattering process increases, and vice versa. We believe that this is the first observation of the contribution of nonequilibrium holes to the reaction at TiO<sub>2</sub>/SCN<sup>-</sup> interfaces.

Generally, the interfacial charge transfer rate has been explained by Marcus theory,<sup>22</sup> which has been adopted to TiO<sub>2</sub>/SCN<sup>-</sup> interfaces and has well explained the charge transfer there.<sup>14,17</sup> In this theory, the charge transfer rate is determined by the difference of the redox potential at the interfaces and the solvent reorganization energy. Reorganization of the solvent molecules always accompanies the molecular vibration; therefore, the maximum of the charge transfer rate is restricted by the molecular vibration rate.<sup>23</sup> For TiO<sub>2</sub>/SCN<sup>-</sup> interfaces, the estimated charge transfer time by Marcus theory is 1.8 ns, and Bahnemann et al.<sup>17</sup> reported that the time constant for the hole transfer process there is 5 μs. Our experimental value of 110–690 fs is much faster than the estimated and reported values, which suggests that the observed hole transfer process is a new-

type transfer process beyond Marcus theory. One possible explanation of the new-type process is nonequilibrium hole transfer before thermalization of the photoexcited energy. It is very exciting to note that the ultrafast nonequilibrium hole transfer in 110–690 fs was observed here because it has been believed that nonequilibrium hole transfer does not occur and only equilibrated holes can be transferred across an interface. This work indicates that the nonequilibrium holes should be taken into account in interface reactions. We believe this result will provide valuable knowledge for designing electrode surfaces and controlling interfacial reactions.

**Acknowledgment.** The authors are grateful to Prof. A. Harata for valuable discussions. This work was supported by Grant-in-Aids for Specially Promoted Research (No. 07102004) and for Scientific Research on Priority Area of Electrochemistry of Ordered Interfaces (No. 09237219) from the Ministry of Education, Science and Culture of Japan.

### References and Notes

- (1) Tributsch, H.; Pohlmann, L. *Science* **1998**, *279*, 1891.
- (2) Nozik, A. J.; Memming, R. *J. Phys. Chem.* **1996**, *100*, 13061.
- (3) Linsebigler, A. L.; Lu, G.; Yate, J. T. *Chem. Rev.* **1995**, *95*, 735.
- (4) Fox, M. A.; Dulay, M. T. *Chem. Rev.* **1993**, *93*, 34.
- (5) Serpone, N.; Pelizzetti, E. *Photocatalysis*; Wiley: New York, 1989.
- (6) Lantz, J. M.; Corn, R. M. *J. Phys. Chem.* **1994**, *98*, 4899.
- (7) Turchi, C. S.; Ollis, D. F. *J. Catal.* **1989**, *119*, 483.
- (8) Bicanic, D. *Photoacoustic and photothermal phenomena*; Springer-Verlag: Berlin, 1992.
- (9) Gomez-Jahn, L. A.; Miller, R. J. D. *J. Chem. Phys.* **1992**, *96*, 3981.
- (10) Marshall, C. D.; Tokmakoff, A.; Fishman, I. M.; Eom, C. B.; Phillips, J. M.; Fayer, M. D. *J. Appl. Phys.* **1993**, *73*, 850.
- (11) Hibara, A.; Morishita, T.; Tsuyumoto, I.; Harata, A.; Kitamori, T.; Sawada, T. *Jpn. J. Appl. Phys.* **1999**, *38*, 2983.
- (12) Morishita, T.; Hibara, A.; Tsuyumoto, I.; Harata, A.; Sawada, T. *Jpn. J. Appl. Phys.*, submitted.
- (13) Hibara, A.; Harata, A.; Sawada, T. *Chem. Phys. Lett.* **1997**, *272*, 1.
- (14) Colombo, D. P.; Bowman, R. M. *J. Phys. Chem.* **1996**, *100*, 18445.
- (15) Colombo, D. P.; Roussel, K. A.; Saeh, J.; Skinner, D. E.; Cavaleri, J. J.; Bowman, R. M. *Chem. Phys. Lett.* **1995**, *232*, 207.
- (16) Colombo, D. P.; Bowman, R. M. *J. Phys. Chem.* **1995**, *99*, 11752.
- (17) Bahnemann, D. W.; Hilgendorff, M.; Memming, R. *J. Phys. Chem. B* **1997**, *101*, 4265.
- (18) Hannappel, T.; Burfeindt, B.; Storck, W.; Willing, F. *J. Phys. Chem. B* **1997**, *101*, 6799.
- (19) Harata, A.; Nishimura, H.; Tanaka, T.; Sawada, T. *Rev. Sci. Instrum.* **1993**, *64*, 618.
- (20) Boudreaux, D. S.; Williams, F.; Nozik, A. J. *J. Appl. Phys.* **1980**, *51*, 2158.
- (21) Kasinski, J. J.; Gomez-Jahn, L. A.; Gracewski, S. M.; Miller, R. J. D. *J. Chem. Phys.* **1989**, *90*, 1253.
- (22) Marcus, R. A. *J. Chem. Phys.* **1956**, *24*, 43966.
- (23) Lanzafame, J. M.; Palese, S.; Wang, D.; Miller, R. J. D.; Meunter, A. A. *J. Phys. Chem.* **1994**, *98*, 11020.